J Math Chem (2010) 47:1145–1153
DOI 10.1007/s10910-009-9651-0

ORIGINAL PAPER

Topographical distance matrices for porous arrays

Andrej Vodopivec · Forrest H. Kaatz · Bohan Mohar

Received: 5 March 2009 / Accepted: 24 November 2009 / Published online: 6 December 2009

Abstract The topographical Wiener index is calculated for two-dimensional graphs describing porous arrays, including bee honeycomb. For tiling in the plane, we model hexagonal, triangular, and square arrays and compare with topological formulas for the Wiener index derived from the distance matrix. The normalized Wiener indices of C_4, T_{13}, and O(4), for hexagonal, triangular, and square arrays are 0.993, 0.995, and 0.985, respectively, indicating that the arrays have smaller bond lengths near the center of the array, since these contribute more to the Wiener index. The normalized Perron root (the first eigenvalue, λ_1), calculated from distance/distance matrices describes an order parameter, $\phi = \lambda_1/n$, where $\phi = 1$ for a linear graph and n is the order of the matrix. This parameter correlates with the convexity of the tessellations. The distributions of the normalized distances for nearest neighbor coordinates are determined from the porous arrays. The distributions range from normal to skewed to multimodal depending on the array. These results introduce some new calculations for 2D graphs of porous arrays.

A. Vodopivec
Department of Mathematics, IMFM, 1000 Ljubljana, Slovenia

F. H. Kaatz
Department of Mathematics and Physics, University of Advancing Technology, Tempe, AZ 85283, USA

F. H. Kaatz (✉)
Department of Mathematics, Chandler-Gilbert Community College, Chandler, AZ 85225, USA
e-mail: fhkaatz@yahoo.com

F. H. Kaatz
Department of Physical Science, Mesa Community College, Mesa, AZ 85202, USA

B. Mohar
Department of Mathematics, Simon Fraser University, Burnaby, BC V5A 1S6, Canada

Keywords Topographical Wiener index · Porous arrays · Distance matrix · Order parameter

1 Introduction

The topological Wiener index has received considerable attention since its introduction [1] in 1947. In an ideal graph all intersite distances are one unit and the sum of all path distances between the vertices is known as the Wiener index. If the sites are represented in a matrix, then the distance matrix is constructed with the shortest distances from site to site, and the Wiener index is then:

$$W(G) = \sum_{i<j} (\mathbf{D}_G)_{ij} \tag{1}$$

where G represents a graph, and $\mathbf{D}_G$ the distance matrix. Hosoya [2] first developed a mathematical formulation of the Wiener index in terms of graph theory in 1971. In this work, we consider the topographical structure of a graph, i.e., the real-space Euclidean distance between sites. This formulation has received considerably less attention [3–6] than the topological nature of a graph, primarily due to the difficulty of determining the 3D length of bonds in real structures.

We consider two-dimensional porous arrays, such as bee honeycomb, and the types most often constructed by scientists in nanotechnology [7]. It is well known [8] that in two dimensions, one can tile the plane by constructing square, triangular, or hexagonal lattices. Porous arrays are examples of all these types of tiling, if one considers the pores as lattice sites and the interpore distance as connecting the lattice in a graph. The pore sites and coordinate positions are determined by Image SXM [9], which assigns coordinate centers based on a best-fitting ellipse. The 2D Wiener index is then:

$$W_{E_{2D}}(G) = \sum_{i<j} \left(D_{E_{2D}}\right)_{ij} \tag{2}$$

where G is the graph in question and E_{2D} refers to the 2D Euclidean index. We note that algorithms [10,11] for determining the computer calculation of the Wiener index have previously been published. The 2D distances were calculated using Excel macros.

2 Methods

For tessellations in the plane, a mathematical algorithm for constructing lattice sites is given by:

$$\vec{a}_1 = a\hat{x} \quad \vec{a}_2 = a\cos\left(\frac{2\pi}{n}\right)\hat{x} + a\sin\left(\frac{2\pi}{n}\right)\hat{y} \tag{3}$$

where a_1 and a_2 are basis vectors for the sites, a is the distance between lattice points, and n is the symmetry of the lattice, 3, 4, or 6. In addition, a 'hexagonal' tiling is

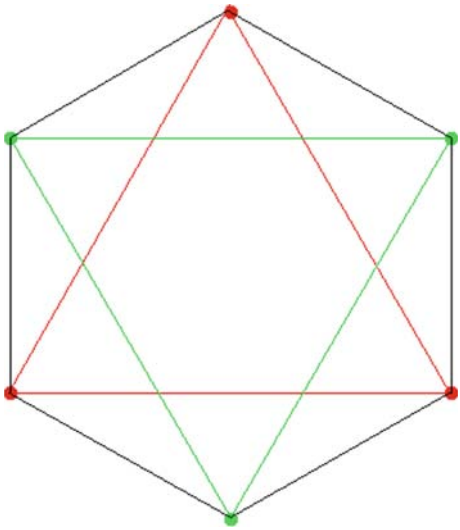

Fig. 1 Hexagonal lattice showing the interconnected triangular symmetry

actually constructed from two interconnected equilateral triangles with a basis shift of the second triangle given by:

$$b_x = a_{1x} + a_{2x} + a \cdot \frac{1}{2} \quad b_y = a_{2y} + a \cdot \frac{\sqrt{3}}{6} \tag{4}$$

where a is again the distance between sites (see Fig. 1). There is some discrepancy between what is called a triangular tiling (six-fold symmetry) and a hexagonal tiling (three-fold symmetry), since the tiles have a different shape than the symmetry of the lattice sites. In this formulation then, bee honeycomb has triangular symmetry (a hexagonal network). We use examples from nanotechnology to represent other tessellations. An example [12] from Choi et al., made from porous anodized aluminum oxide, is also triangular, an example [13] from Krishnan et al., also made from anodized aluminum oxide, has square symmetry, and an example [14] from Hulteen et al., fabricated by 'nanosphere lithography' has hexagonal symmetry.

In our analysis, we also look at an order parameter ϕ, which measures [17,18] the 'folding' of a linear array. This parameter is defined by the Perron root (the first eigenvalue, λ_1), calculated from distance/distance (**D/D**) matrices, $\phi = \lambda_1/n$, where $\phi = 1$ for a linear graph and n is the order of the matrix. **D/D** matrices are defined by:

$$(\mathbf{D}/\mathbf{D})_{ij} = \frac{(\mathbf{D}_E)_{ij}}{(\mathbf{D}_{E_{2D}} + \mathbf{I})_{ij}} \tag{5}$$

where $\mathbf{D}_E$ is the topographical direct Euclidean distance between lattice sites (not path dependent) and $\mathbf{D}_{E_{2D}}$ is the Euclidean distance matrix in two dimensions. The entries of the **D/D** matrices are thus always ≤ 1. The eigenvalues are determined in the usual way:

$$P(\lambda) = \det(\mathbf{D}/\mathbf{D} - \lambda\mathbf{I}) = 0 \tag{6}$$

where **I** is the identity matrix, and λ an eigenvalue. The Perron root is the largest eigenvalue from these **D/D** matrices and the order parameter ϕ gives a measure of the convexity of the basic unit of tiling in two dimensions.

We use the computer algebra software, Maxima [15], to generate graphs of the porous arrays, and to determine the topographical Wiener index. A separate Lisp program was written [16] by one of the authors using previous algorithms for the Wiener index and to generate the graphs. Maxima was also used for matrix analysis and to determine eigenvalues.

3 Results

There has been extensive progress in the study of topological indices in recent years with the result that formulas for the Wiener index of many types of graphs have been determined. For tiling in the plane, the relevant equations were published in the last five to ten years. We have two examples of triangular graphs, one from bee honeycomb, where parameters establishing the amount of order in the arrays were recently [19,20] determined, and one example from nanotechnology, Choi et al. For a triangular array, the equation [21] we use is:

$$\boldsymbol{W_T}(m) = \frac{1}{40} m(m+1)(m+2)(m+3)(2m+3) \tag{7}$$

where m is the number of 'bonds' between lattice points in the graph. We use successively larger triangles T_1, T_4, T_7, T_{10}, and T_{13}, where the smaller triangles are nested within the larger ones. A graph of the array T_{13}, as generated by Maxima, is shown in Fig. 2a, and is the same for both triangular arrays. This creates the sequence of numbers, 3, 231, 2142, 9867, and 31668 for $m = 1$, 4, 7, 10, and 13, as shown in Table 1. The corresponding topographical Wiener index for bee honeycomb HC1060, and the nanoarray from Choi et al. is listed along with the normalized values (with respect to the topological index). Since the Wiener index is a measure of the 'compactness' of a graph, we see that since the normalized values are all less than one, the 'bonds' near the center of the array must have shorter values than the mean value of all the bonds. The bonds near the center contribute more to the aggregate total in the Wiener index, so on average they are less than one.

For a square array, the equation for an octagonal square-cell configuration [22] with n circular levels is:

$$\boldsymbol{W_S}(O(n)) = \frac{211n^5}{5} - \frac{181n^4}{3} + \frac{109n^3}{3} - \frac{35n^2}{3} + \frac{22n}{15} \tag{8}$$

where $n \geq 2$. This generates the sequence 632, 6248, 29912, for $n = 2$, 3, and 4. We include the value 8 for a unit square cell in Table 1, as well. The octagonal array from Maxima is shown in Fig. 2b. As before, the normalized topographical Wiener index is less than one, with the same implications.

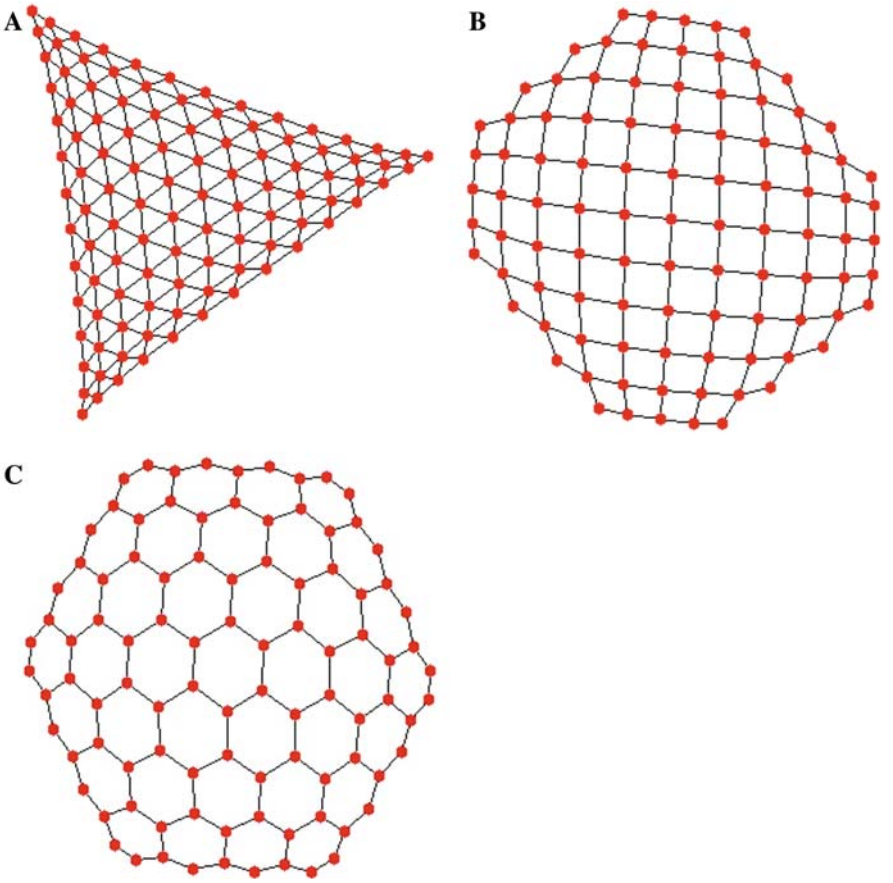

Fig. 2 **a** Graph of the Maxima figure for the honeycomb (HC) and Choi T_{13} arrays. **b** Graph of the Maxima figure for the square O(4) array from Krishnan et al. **c** Graph of the Maxima figure for the Hulteen et al. C_4 array

The example for hexagonal arrays, where the sites actually have three-fold symmetry comes from a nanoarray created with nanosphere lithography. In this procedure, latex spheres are placed on a substrate and material is deposited in interstitial sites to form nanoarrays. The spheres then form a hexagonal close packed array and the material in the interstitial sites form the lattice points of the graph. The equation for the Wiener index has been determined [23,24] and is:

$$W_H(n) = \frac{1}{5}(164n^5 - 30n^3 + n) \tag{9}$$

where n is the number of hexagonal cells on a side. This equation gives the sequence 27, 1002, 7809, and 33204, for $n = 1$, 2, 3, and 4. The normalized index is also less than one as before. A graph of the array C_4 from Maxima is shown in Fig. 2c.

Table 1 Topographical and topological Wiener indices for various porous arrays

Array	Wiener index	Topographical index	Normalized
HC1060T1	3	3.0	1.0
HC1060T4	231	230.5722	0.998
HC1060T7	2142	2136.5718	0.997
HC1060T10	9867	9832.3762	0.996
HC1060T13	31668	31517.3149	0.995
ChoiT1	3	3.0	1.0
ChoiT4	231	230.3991	0.997
ChoiT7	2142	2134.0342	0.996
ChoiT10	9867	9835.7314	0.997
ChoiT13	31668	31562.9932	0.997
KrishnanO1	8	7.9767	0.997
KrishnanO2	632	626.5753	0.991
KrishnanO3	6248	6170.9084	0.988
KrishnanO4	29912	29465.6564	0.985
HulteenC1	27	26.8863	0.996
HulteenC2	1002	999.9226	0.998
HulteenC3	7809	7772.8189	0.995
HulteenC4	33204	32978.1412	0.993

The distance/distance matrices can be compared for the three types of tiling in the plane, i.e., a triangle, square, and hexagon. We comment that the closed graph of the basic unit of tiling has the same order parameter, ϕ, as a graph with one side missing, so that ϕ actually measures the degree of 'folding' or convexity of the tile. Since the **D/D** matrices are symmetric, they have real eigenvalues with one positive (Perron) root and the rest negative. We compare the ideal three tiling units with coordinates from porous arrays, the results of which are summarized in Table 2. For the square array the experimental **D/D** matrix is calculated as:

$$\mathbf{D}/\mathbf{D}_{\text{exp}} = \begin{bmatrix} 0 & 1.0 & 1.0 & 0.7286855 \\ 1.0 & 0 & 0.6929103 & 1.0 \\ 1.0 & 0.6929103 & 0 & 1.0 \\ 0.7286855 & 1.0 & 1.0 & 0 \end{bmatrix}$$

while for the model square array of the graph it is:

$$\mathbf{D}/\mathbf{D}_{\text{model}} = \begin{bmatrix} 0 & 1 & 1 & 0.7071068 \\ 1 & 0 & 0.7071068 & 1 \\ 1 & 0.7071068 & 0 & 1 \\ 0.7071068 & 1 & 1 & 0 \end{bmatrix}.$$

Table 2 Perron eigenvalues and order parameters for basic units of tiling

Array	Perron eigenvalue λ_1	ϕ
Triangle (exp)	2	0.6667
Triangle (model)	2	0.6667
Square (exp)	2.71088	0.6777
Square (model)	2.7071	0.6768
Hexagon (exp)	4.407067	0.7345
Hexagon (model)	4.3987	0.7331

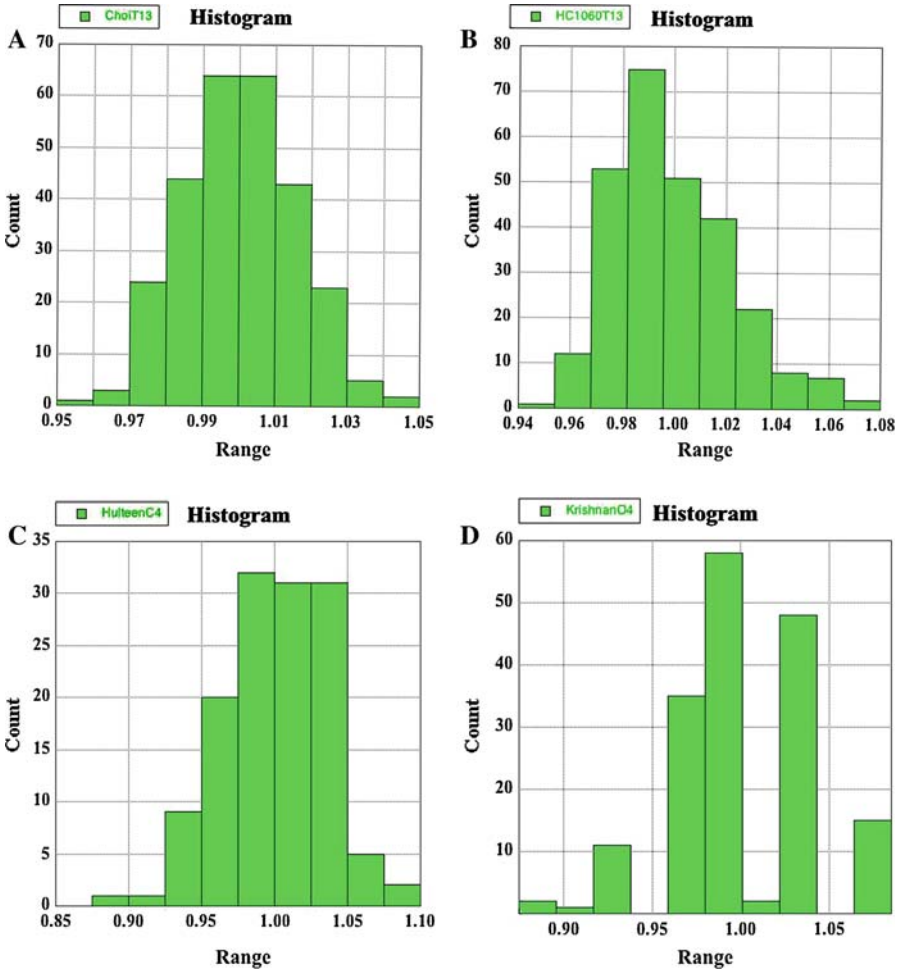

Fig. 3 **a** Normal distribution from the Choi T_{13} array. **b** Skewed distribution from the honeycomb (HC) array. **c** Distribution from the Hulteen C_4 array. **d** Multimodal distribution from the Krishnan O(4) array

Table 3 Statistics for the distributions of the porous arrays

Array	Min	Max	Points	Median	SD	Skewness
HC1060T13	0.9528893	1.068543	273	0.995730	0.02280767	0.7090689
ChoiT13	0.9576133	1.047158	273	1.000124	0.01547439	0.113267
KrishnanO4	0.8937172	1.067651	172	0.9972413	0.03816923	−0.322736
HulteenC4	0.8950636	1.087623	132	1.006131	0.03624411	−0.167567

From Table 2, we see that the hexagon is the most linear of the structures, in agreement with the recent proof [25] of the honeycomb conjecture, which states that any partition of the plane into regions of equal area has perimeter at least that of the regular hexagonal honeycomb tiling. We also note that the experimental square and hexagonal arrays are more linear than their model counterparts, and that the triangular tiling has no change.

The histograms of the normalized distances are shown in Fig. 3. The normalization is such that, after the intersite distances are summed, each distance is divided by the mean. Thus the mean of the normalized arrays is 1.0. The statistics of these distances between lattice points are given in Table 3. The distribution from Choi et al., in shown in Fig. 3a. It is a normal-centered distribution, with a median slightly more than one, standard deviation 0.015 and skewness of 0.11. Skewness is a measure of the asymmetry of a distribution and can be expressed as:

$$\gamma_1 = \frac{1}{n} \frac{\sum_{i=1}^{n} (x_i - \bar{x})^3}{s^3} \tag{10}$$

or the third moment about the mean, where s is the standard deviation, and n is the number of data points.

In Fig. 3b we show the distribution from the honeycomb (HC) array. It is skewed to the right, with a median slightly less than one, standard deviation 0.023 and skewness 0.709. Figure 3c shows the histogram from Hulteen et al., and is skewed to the left, with a median greater than one, while Fig. 3d shows the multimodal histogram from Krishnan et al., and is also skewed to the left, with a median less than one.

4 Conclusion

In summary, we have introduced new results for the topographical Wiener index and distance matrices for porous arrays. There are now numerous examples of experimental 2D arrays, many of which could be analyzed in the manner described in this manuscript. Tiling in the plane is accomplished by triangular, hexagonal and square arrays and the topographical Wiener indices have been determined for several porous arrays. We have also presented figures of the distributions of these arrays and their statistics. We have used commonly available software to achieve these goals.

Acknowledgments An iMac @ 2.4 GHz with Mac OS X 10.5.6 was used in this analysis. The Lisp program written for Maxima is designed for version 5.16.3. Image SXM is a free download for the Max OS. We thank the referee for comments that improved the clarity of the manuscript.

References

1. H. Wiener, Structural determination of paraffin boiling points. J. Am. Chem. Soc. **69**, 17–20 (1947)
2. H. Hosoya, Topological index. A newly proposed quantity characterizing the topological nature of structural isomers of saturated hydrocarbons. Bull. Chem. Soc. Jpn. **44**, 2332–2339 (1971)
3. B. Bogdanov, S. Nikolic, N. Trinajstic, On the three-dimensional Wiener number. J. Math. Chem. **3**, 299–309 (1989)
4. Z. Mihalic, N. Trinajstic, The algebraic modeling of chemical structures: on the development of three-dimensional molecular descriptors. J. Mol. Struct. (Theochem) **232**, 65–78 (1991)
5. S. Nikolic, N. Trinajstic, Z. Mihalic, S. Carter, On the geometric-distance matrix and the corresponding structural invariants of molecular systems. Chem. Phys. Lett. **179**, 21–28 (1991)
6. Z. Mihalic, S. Nikolic, N. Trinajstic, Comparative study of molecular descriptors derived from the distance matrix. J. Chem. Inf. Comput. Sci. **32**, 28–37 (1992)
7. H. Masuda, H. Asoh, M. Watanabe, K. Nishio, M. Nakao, T. Tamamura, Square and triangular nanohole array architectures in anodic alumina. Adv. Mater. **13**(3), 189–192 (2001)
8. L.F. Toth, *Regular Figures* (MacMillan, New York, 1964), pp. 21–38
9. The website of Image SXM: http://www.liv.ac.uk/~sdb/ImageSXM
10. B. Mohar, T. Pisanski, How to compute the Wiener index of a graph. J. Math. Chem. **2**, 267–277 (1988)
11. M. Juvan, B. Mohar, Bond contributions to the Wiener index. J. Chem. Inf. Comput. Sci. **35**, 217–219 (1995)
12. J. Choi, Y. Luo, R.B. Wehrspohn, R. Hillebrand, J. Schilling, U. Gösele, Perfect two-dimensional porous alumina photonic crystals with duplex oxide layers. J. Appl. Phys. **94**(8), 4757–4762 (2003)
13. R. Krishnan, H.Q. Nguyen, C.V. Thompson, W.K. Choi, Y.L. Foo, Wafer-level ordered arrays of aligned carbon nanotubes with controlled size and spacing on silicon. Nanotechnology **16**, 841–845 (2005)
14. J.C. Hulteen, D.A. Treichel, M.T. Smith, M.L. Duval, T.R. Jensen, R.P. Van Duyne, Nanosphere lithography: size-tunable silver nanoparticle and surface cluster arrays. J. Phys. Chem. B **103**, 3854–3863 (1999)
15. M. Randic, M. Vracko, On the similarity of DNA primary sequences. J. Chem. Inf. Comput. Sci. **40**, 599–606 (2000)
16. M. Randic, A.F. Kleiner, L.M. DeAlba, Distance/distance matrices. J. Chem. Inf. Comput. Sci. **34**, 277–286 (1994)
17. The website for Maxima: http://www.maxima.sourceforge.net
18. Contact one of the authors at andrej.vodopivec@gmail.com for more information on the Lisp program
19. F.H. Kaatz, A. Bultheel, T. Egami, Order parameters from image analysis: a honeycomb example. Naturwissenschaften **95**(11), 1033–1040 (2008)
20. F.H. Kaatz, A. Bultheel, T. Egami, Real and reciprocal space order parameters for porous arrays from image analysis. J. Mater. Sci. **44**, 40–46 (2009)
21. W.C. Shiu, P.C.B. Lam, K.K. Poon, On Wiener numbers of polygonal nets. Discret. Appl. Math. **122**, 251–261 (2002)
22. I. Gutman, S. Klavzar, A. Rajapakse, Average distances in square-cell configurations. Int. J. Quan. Chem. **76**, 611–617 (1999)
23. B.Y. Yang, Y.N. Yeh, A crowning moment for Wiener indices. Stud. Appl. Math. **112**, 333–340 (2004)
24. W.C. Shiu, P.C.B. Lam, The Wiener number of the hexagonal net. Discret. Appl. Math. **73**, 101–111 (1997)
25. T.C. Hales, The honeycomb conjecture. Discret. Comput. Geom. **25**, 1–22 (2001)